ELSEVIER

Mechanical behavior and damage evolution in E-glass vinyl ester and carbon composites subjected to static and blast loads

Srinivasan Arjun Tekalur [a], Kunigal Shivakumar [b], Arun Shukla [a,*]

[a] Dynamic Photomechanics Laboratory, Department of Mechanical Engineering and Applied Mechanics, University of Rhode Island, Kingston, RI, USA
[b] Center for Composite Materials Research, Department of Mechanical and Chemical Engineering, North Carolina A&T State University, Greensboro, NC, USA

Abstract

Fiber based composites have found extensive applications in various fields. In this study, two different fiber materials, namely, E-glass and carbon, with different architecture are chosen. Polymer (vinyl ester) based composites were designed using these fibers and were fabricated using VARTM process. These composites were subjected to quasi-static and high strain rates of loading utilizing different testing methodologies. In quasi-static testing, the tensile, compressive and shear properties were studied using existing ASTM standard testing procedures and the results are reported. The carbon composite showed higher tensile and compressive modulus. In-plane shear properties of both the composites were comparable and inter laminar shear properties of E-glass composites were observed to be better than the carbon composite because of the better nesting between the E-glass fabric layers. A shock tube and a controlled explosion tube were utilized in the study of dynamic damage behavior of these composite materials. Based on the experimental study, it is observed that the carbon fiber composites tend to achieve sudden destructive damage whereas E-glass fiber composites tend to sustain progressive damage, under dynamic loading.
© 2007 Elsevier Ltd. All rights reserved.

Keywords: A. Polymer–matrix composites (PMCs); B. Mechanical properties; C. Damage mechanics; E. Resin transfer moulding (RTM); Blast loading

1. Introduction

Composite materials have replaced metals in various engineering applications owing to their numerous advantages, like high strength/weight ratio, low cost, better stealth properties, etc. Due to these advantages, there is an increasing demand for use of these materials in defense applications like naval ships, warplanes, armor vehicles and re-entry vehicles. Conventionally, metal-based materials were used in these applications and studies exist in the literature [1,2] that characterizes the structural behavior of these materials when subjected to blast loadings. With an increasing use of composites, to achieve their optimum performance, a thorough understanding of material and damage behavior of these composites is necessary. In recent times, E-glass and carbon fiber based composites have found extensive use in naval structures and there are various studies in the literature [3–5], which intend to characterize these materials under different quasi-static and ballistic loadings. But, often these materials are subjected to blast loadings occurring from warheads and torpedoes during service or regular war exercises. Computational studies [6,7] provide theoretical prediction of response of composite materials to blast type loadings, under some simplifying assumptions. The response of these composite to such types of explosive and air blast are complex to model and are less studied experimentally. In the present work, the damage progression in E-glass/vinyl ester and carbon fiber/vinyl ester composites are experimentally studied under both quasi-static and dynamic loading rates. Based on the study, comparisons are made between the performances of these composites when exposed to high loading rates.

* Corresponding author.
 E-mail address: shuklaa@egr.uri.edu (A. Shukla).

2. Materials

Two different fiber architectures, namely, woven roving glass and stitch bonded carbon fibers were chosen for the study. The resin system used was Dow Chemical's Derakane 510A-40. Details of these materials are given below.

2.1. Glass fibers

A combination of good mechanical properties and relatively low cost makes glass fiber attractive choice for the marine structures. The glass fabric chosen was woven roving E-glass supplied by Fiber Glass Industries' (FGI) and designated as FGI-1854 [8]. Glass fibers had Super 317 sizing for ease of handling, fast wet out, and compatibility with a number of resins including vinyl ester. The areal weight was 610 g/m^2 (18 oz/sqyd) with an unbalanced construction having 59% and 41% of fibers in warp and fill directions, respectively. This ratio was verified by the pic count (i.e. the number of rovings per inch). The fabric architecture is shown in Fig. 1a.

2.2. Carbon fibers

The carbon stitch bonded fabric designated by LT650-C10-R2VE was supplied by Devold AMT AS, Sweden. This fabric is abbreviated as Devold LT650 fiber. This was an equi-biaxial fabric produced using Toray's Torayca T700 12k carbon fiber tow with a vinyl ester compatible sizing (FOE). The areal weight of the fabric was 634 g/m^2 with 315 g/m^2 of fiber in the 0° direction and 305 g/m^2 in the 90° direction. Both the directional fibers were stitched with a 14 g/m^2 polyester knitting thread [9]. Toray's Torayca T700 carbon fiber was chosen because of lower cost and higher fracture strain. The T700 fiber has a tensile strength of 4.9 GPa (711 ksi), modulus of 230 GPa (33.4 Msi) and an elongation of 2.1%. Fig. 1b illustrates the architecture of the front and back surfaces.

2.3. Resin

The matrix used was Dow Chemical's Derakane 510A-40 [10], a brominated vinyl ester, formulated for the vacuum assisted resin transfer molding (VARTM) process. The bromination imparts a fire resistant property to the composite. It has higher fracture strain than typical polyesters and hence produces composites with superior mechanical properties, impact resistance, and fatigue life. The vinyl ester has a viscosity of 350 cps and is ideal for the VARTM process. It can be catalyzed to give a wide range of cure times. The matrix specific gravity is 1.23; tensile modulus and strength are about 3.4 GPa (0.5 Msi) and 73 MPa (10.5 ksi), respectively; flexural modulus and strength are about 3.6 GPa (0.53 Msi) and 125 MPa (18 ksi), respectively; and heat distortion temperature is 225 °F.

3. Panel fabrication

Composite panels of size 600 × 900 mm (2 × 3 ft) and 2.5 mm (0.1 in.) thickness were fabricated by the VARTM process. To achieve 2.5 mm nominal thickness, six plies of FGI-1854 Rovcloth and four plies of Devold LT 650 fabrics were used. All fabrics were cut and stacked in the 0° (warp) direction with the warp face down so that specimens in 0° (X_1) and 90° (X_2) directions could be extracted to determine the basic mechanical properties. The preforms were protected from dirt, grease or other contaminants that may prevent layer bonding during consolidation. Details of the VARTM process are explained in references [11–13]. The post-cured panels were inspected visually for surface defects and tap tested [14] for delaminations. All panels were found to be free from surface defects and delaminations. There were no dry fiber regions or voids and the fibers were not deformed to any other shape than by vacuum compression during molding. The uniformity of the panels was verified by measuring the thickness of all test coupons and found to have less than 5% variation.

3.1. Fiber volume fraction

The fiber volumes of the composite panels are listed in Table 1. The fiber volumes of FGI-1854 glass panels were obtained using both the areal density method and the matrix burn off test according to ASTM D3171-99 [15]. The fiber volume of FGI-1854 is 60.5% by the areal density method and 58.7% by the matrix burn-off method. Majority of this 1.8% difference may be due to the burn off of the fiber sizing. The fiber volume of Devold LT-650 is 58% by the areal density method and that includes 2.2% weight of the polyester stitch fiber. The fiber volume obtained for the
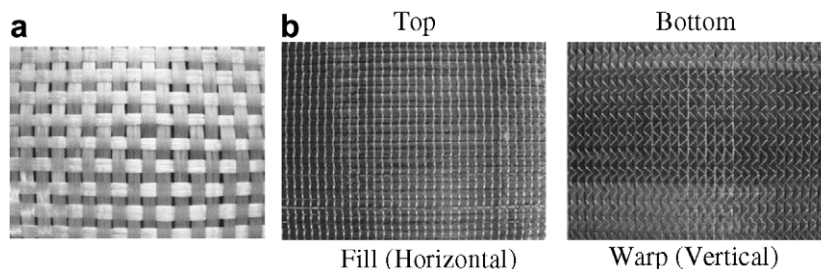

Fig. 1. Fiber architectures: (a) FGI's 1854 glass fabric (warp-vertical direction). (b) Devold LT650 T700 carbon.

Table 1
Fiber volume fractions

Material	Fiber volume fraction, V_F (%)			
	Matrix burn-off method	Areal density method		Density (g/cm³)
FGI-1854	58.7	60.5	60.5[a]	1.98
Carbon LT650		58.0	55.8[a]	1.57

[a] After discounting polyester thread.

FGI-1854 woven roving glass and Devold LT650 fabrics are quite good. Fiber volume and composite's densities are listed in Table 1.

4. Static mechanical characterization

Static tension, compression, in-plane shear and inter-laminar shear properties were measured as per the Refs. [12,13]. A summary of test and results are given below.

4.1. Tension properties

Tension properties were measured using ASTM Standard Test Method (D 3039/D 3039M-00) for Tensile Properties of Polymer Matrix Composite Materials. From the test data, tensile modulus, strength, and Poisson's ratio were determined. Five specimens were tested in each of the warp (X_1) and fill (X_2) directions. The average values and the standard deviations were calculated and are listed in Table 2. The consistency and minimal data scatter confirmed the quality of the panel fabrication, specimen preparation, testing, and data reduction.

The woven roving glass composite has a higher stiffness in the X_1-direction than in the X_2-direction because of

Table 2
Summary of mechanical properties of composites

Properties			FGI-1854	Carbon LT650
Volume fraction of fiber V_F (%)			60.5	55.8
Tension	Strength (MPa)	X_1	512.5 (22.5)[a]	1125.7 (23.4)
		X_2	350.9 (8.9)	1036.9 (26.3)
	Modulus (GPa)	X_1	29.2 (1.8)	56.7 (1.1)
		X_2	23.9 (1.9)	57.1 (2.1)
	Poisson's ratio	X_1	0.16 (0.01)	0.07 (0.006)
		X_2	0.14 (0.003)	0.04 (0.001)
Compression	Strength (MPa)	X_1	363.4 (75.0)	449.7 (37.6)
		X_2	336.4 (25.2)	387.2 (28.2)
	Modulus (GPa)	X_1	31.9	67.5
		X_2	26.9	59.1
In-plane shear	0.2% offset strength (MPa)	X_1	44.7 (0.6)	47.5 (0.7)
		X_2	47.3 (5.9)	45.0
	Modulus (GPa)	X_1	4.5 (0.3)	4.2 (0.4)
		X_2	4.3 (0.6)	3.9
Inter-laminar shear strength (MPa)		X_1	77.1 (1.0)	59.3 (2.6)
		X_2	58.4 (1.4)	54.3 (2.2)

X_1 – warp direction and X_2 – fill direction.
[a] Standard deviation.

higher percent of fibers in the X_1-direction and higher number of crimps in the X_2-direction. The average tensile modulus and the strength of the FGI-1854 woven rovings are 29.2 GPa and 512.5 MPa, respectively in the warp (X_1) direction and 23.9 GPa and 350.9 MPa, respectively in the fill (X_2) direction.

The tensile modulus and the strength of Devold LT650 in warp (X_1) direction are 56.7 GPa and 1125.7 MPa, respectively and in the fill (X_2) direction are 57.1 GPa and 1036.9 MPa, respectively. Because of the balanced construction in the warp and the fill directions, the properties are nearly equal. The higher modulus of carbon fibers naturally gives rise to higher mechanical properties for these composites compared to the glass composites. The stitch bonded carbon composites when compared to the glass woven roving have more than twice the tensile modulus and the strength. The straightness of the fiber is also the reason for the superior performance of the carbon composites.

The Poisson's ratio of all the composites is lower because of the orthogonal fiber architecture. The Poisson's ratios of the glass fabrics ranged between 0.14 and 0.16 while the carbon fiber composite ranged between 0.04 and 0.07.

4.2. Compression properties

Compression properties were measured using ASTM Standard Test Method (D 3410/D 3410M – 95) for Compressive Properties of Polymer Matrix Composite Materials with Unsupported Gage Section by Shear Loading. The compression modulus and strength of all the specimens were calculated and the average values and the standard deviations are listed in Table 2.

The Devold LT650 had the best compression properties among the three fiber systems considered. The compression strength depends on the matrix and the fiber sizing (fiber–matrix adhesion). If the adhesion were the same for all of the fibers, the compression strength is expected to be nearly same for same wave length of fiber architecture and stitch density. Because of the straightness of the Devold LT650 fibers, the compression strength is about 15% more than the glass composite. Furthermore, the FOE sizing on carbon fibers appears to offer a good adhesion between the carbon and vinyl ester, thus contributing to the superior compression strength. The compression modulus is higher than the tensile modulus for both the composite systems. The compression modulus and the strength of the FGI-1854 woven rovings are 31.9 GPa and 363.4 MPa, respectively in the warp (X_1) direction and 26.9 GPa and 336.4 MPa, respectively in the fill (X_2) direction. The compression modulus and the strength of Devold LT650 in warp (X_1) direction are 67.5 GPa and 449.7 MPa, respectively and in the fill (X_2) direction are 59.1 GPa and 387.2 MPa, respectively. The compression modulus of the Devold LT650 composite is more than twice that of the FGI-1854 composite.

4.3. In-plane shear properties

In-plane shear tests were conducted using an Iosipescu test fixture [15]. During the test the strain gages went off-scale at around 1.8% shear strain and hence the shear strength at 5% shear strain was not determined. The shear modulus G_{12} was determined from the initial slope of the shear stress versus strain plot. The 0.2% offset shear strength was determined by the intersection of a line parallel to initial slope and offset by 0.2% shear strain from the origin. The average and the standard deviation of shear modulus and 0.2% offset shear strength are listed in Table 2.

The in-plane shear modulus and the 0.2% offset strength of the FGI-1854 woven rovings are 4.5 GPa and 44.7 MPa, respectively in the warp (X_1) direction and 4.3 GPa and 47.3 MPa, respectively in the fill (X_2) direction. The in-plane shear modulus and the 0.2% offset strength of Devold LT650 in warp (X_1) direction are 4.2 GPa and 47.5 MPa, respectively and in the fill (X_2) direction are 3.9 GPa and 45.0 MPa, respectively.

4.4. Inter-laminar shear strength (ILSS)

Tests were conducted using the modified short beam shear test [16]. The ILSS was calculated from the failure load. The average and the standard deviation values of ILSS are listed in Table 2. The FGI-1854 has the higher (77 MPa and 58.4 MPa) shear strength because of the better nesting between the fabric layers whereas the Devold LT650 (59.3 MPa and 54.3 MPa) has lower values because of its lower fabric nesting. The ILSS of Devold LT650 is 77% of the FGI-1854 in the X_1-direction and 93% of the FGI-1854 in the X_2-direction.

5. Thermal decomposition characterization

Thermal decomposition was carried out in inert nitrogen atmosphere to study the volatile contact and also in oxidizing atmosphere (air) to study oxidative decomposition. Specimens (22.9 mm diameter) of neat resin (5.1 mm thick), FGI-1854 and Devold LT-650 composites (2.5 mm thick) were prepared. The specimens were dried at 60 °C for 24 h to remove absorbed moisture and then stored in a desiccator until ready for use. Specimens were placed in individual uncovered alumina crucibles and weighed. Weights for the empty crucibles were also recorded. The crucibles were placed into the bottom of a 950 °C Lindberg Retort-Equipped Furnace, which was preheated to 50 °C. The temperature controller of the Lindberg Furnace was programmed with a ramp rate of 300 °C/h to a set point of 850 °C with no hold time and then set to quickly cool to 50 °C after reaching 850 °C. The retort door was sealed before starting each test. The purge gas was adjusted for 28×10^3 cm^3/h @ 16–19 mm of H_2O and the thermal test was started. Test #1 used N_2 blanketing gas for the entire program cycle (ramp-up & cool-down). Test #2 used Air blanketing gas for the ramp-up and N_2 for the cool-down

Table 3
Residual weight percent after thermal decomposition

Material	Char yield %	
	Test #1 (in N_2)	Test #2 (in air)
Neat VE	13.5	3.7
FGI-1854 + VE	73.1	68.5
Devold LT650 + VE	67.2	51.0

to arrest any further oxidation of the specimens. Samples were held at 50 °C to keep them dry until ready for weighing. The percent residual weights are listed in Table 3.

Tests run in N_2 resulted in higher char yield for all the three specimen types than tests run in air. In N_2 atmosphere, weight loss is entirely due to vaporization of volatiles in the matrix while in air the weight loss includes oxidation of carbon char and carbon fibers.

6. Blast loading experiments

Two materials, namely, E-glass (FGI-1854) and carbon fibers (Devold LT650) composites were subjected to blast loading and their performances are reported below. Dynamic blast loads can be obtained from different laboratory sources. A shock tube can produce the air blast alone while an actual explosive could induce burning in the material in addition to the air blast. Square panels made of the composite materials were subjected to shock blast covering a diameter of 75 mm (3 in.) and explosive blast from a controlled explosion tube (CET) covering a diameter of 25 mm (1 in.). The loading, panel strain response and failure modes were recorded and described.

6.1. Shock blast load

6.1.1. Shock tube – brief theory and construction

A shock tube is used to generate a gas flow with conditions which are difficult to generate in other test devices, although they are only achieved for a very short amount of time. In its simplest form a shock tube consists of a long rigid cylinder, divided into a high-pressure driver section and a low pressure driven section, which are separated by a diaphragm. The tube is operated by pressurizing the high-pressure section until the pressure difference across the diaphragm reaches a critical value and it ruptures. This rapid release of gas creates a shock wave that travels down the tube to impart air blast loading on a specimen.

A brief schematic of the shock tube facility at the University of Rhode Island is shown in Fig. 2a. The driver and driven sections have a .15 m (6 in.) inner diameter and the converging section begins as .15 m (6 in.) in diameter and ends as .07 m (3 in.). The driver gas is helium for its lightweight, nonexplosive nature, low cost, and availability. The driven gas is the ambient air of the environment.

The shock tube is instrumented with pressure and velocity measurements to provide real time data about the shock
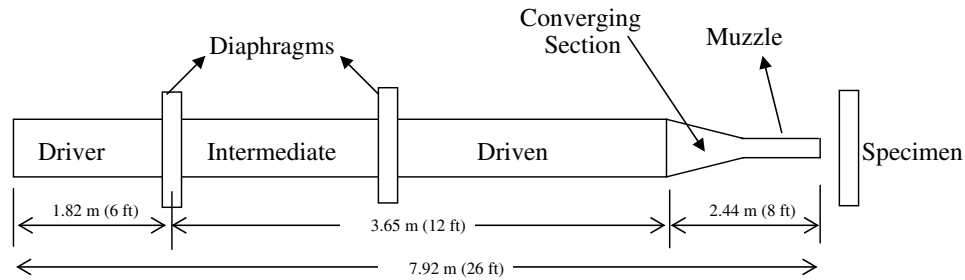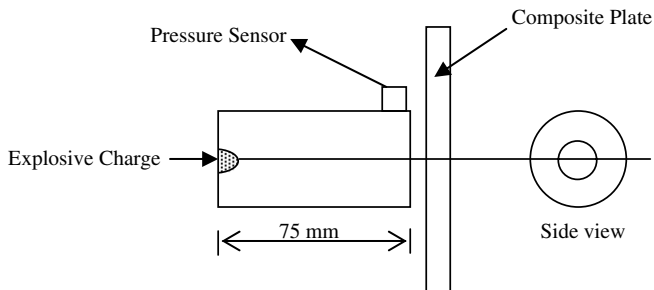
Fig. 2a. Schematic of the shock tube.

Fig. 2b. Schematic of the controlled explosion tube.

pressure and shock velocity. A PCB 134A23 dynamic pressure sensor is mounted at the muzzle section of the shock tube and graphite rods are used as break circuit initiators to measure the shock velocity. The driver pressure can also be measured for calibration purposes. Thin mylar sheets (10 mil) are used as diaphragm material in the shock blast experiments. The driver pressure and hence the shock pressure obtained from the burst of these diaphragms are controlled by number of plies of sheets used. A typical loading history obtained from shock tube is plotted in Fig. 3. The first peak pressures obtained in such experiments are quoted as the "input shock pressure" or just the shock pressure to which the specimen are subjected to. This remains constant for given number of mylar diaphragms. The second peak is the "reflected shock pressure" from

Fig. 3. Typical shock pressure – time profiles obtained in the shock tube. Shown here is the shock pressure history for 3 plies of 10 mil mylar diaphragm.

the specimen that the shock blast is impinged upon. This is dependent on the material and boundary condition of the specimen. Typically this can vary between 1.5 and 3 times the shock pressure and were recorded for all the experiments in this study.

6.2. Specimen

The specimens used for shock blast study were 305 mm (12 in.) square plates of 2.5 mm (0.1 in.) thickness. These plates were fixed on all ends using rigid clamping fixture which exposed a square area of 228 mm × 228 mm (9 in. × 9 in.) to the shock blast. The muzzle of the shock tube was flushed against the plate. The plates were also instrumented with strain gages on the rear surface at two different points along the centerline of the specimen and 2 in. away from the center point, and outside the area of blast. One of the strain gages was in the vertical direction (X_2) and the other in the horizontal direction (X_1). A schematic of the specimen is shown in Fig. 4.

6.3. Results

Damage in FGI-1854 glass/vinyl ester composites under dynamic blast conditions were observed and examined. The panels were subjected to increasing level of shock loading by varying the driven pressure in the shock tube. The input shock pressure varied from 0.2 MPa (30 psi) to 0.8 MPa (116 psi). Fig. 5 shows the damage progression in the plates as they were subjected to increasing shock pressures, quoted in the inset. The shock loading induced visual damage in the center and along the boundary regions. The spread and area of these damage regions increased as we increased the input shock pressure. These panels also endured permanent deformation due to the shock. To measure the magnitude of this permanent deformation, a laser displacement sensor and an automated table were used. The data obtained from the sensor was plotted as deformation profiles. A typical profile obtained for a panel subjected to 0.5 MPa (72.5 psi) shock pressure, is shown in Fig. 6. The maximum deflection was at the center and reduced gradually towards the fixed boundaries. Axisymmetric nature of the loading and nearly balanced composite materials produced concentric contours of permanent
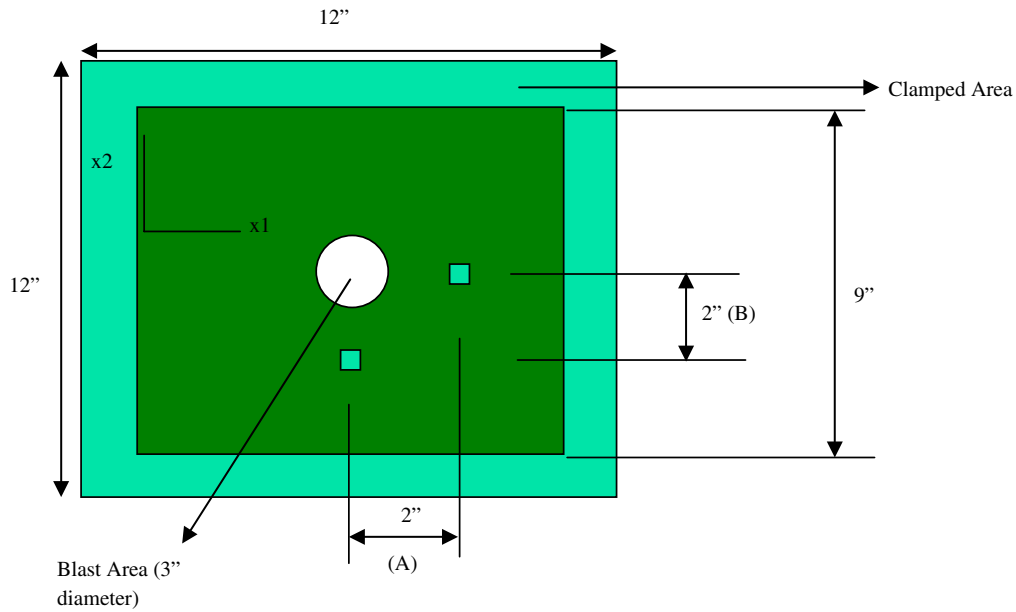
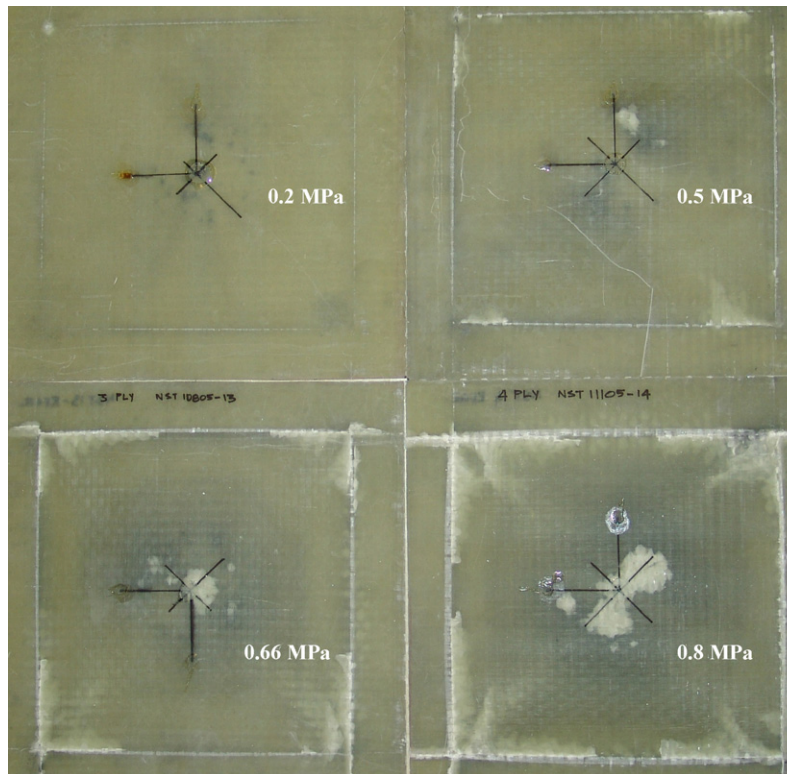Fig. 4. Schematic of the specimen for the shock tube testing.

Fig. 5. Damage progression in E-glass/vinyl ester composites, subjected to shock blast loading. Shown here is the rear face of the panels with shock levels in inset.

deformation. Fig. 7 plots the maximum deformation value for each panel corresponding to the input shock level that the panel was subjected. The magnitude of this deformation increases as the input shock level is increased.

Panels of Devold LT650 composites were subjected to similar shock pressures as used for FGI-1854. The mode

of damage in these panels was significantly different from those observed before in the FGI-1854 panels. Fig. 8 shows the damage behavior of these panels. As seen, these panels tend to resist damage until a certain level of input shock pressure (0.6 MPa), which can be referred as ''threshold'' pressure. After this threshold level, extensive delaminations
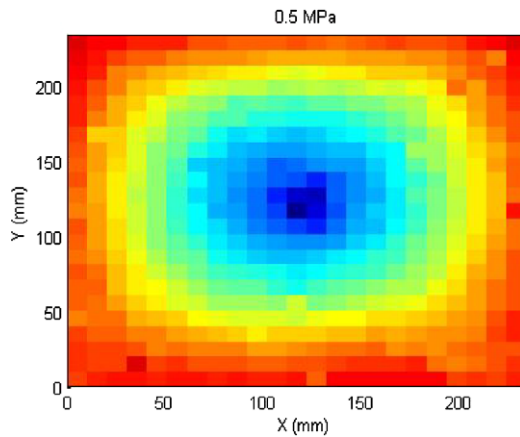
Fig. 6. Typical profile of permanent deformation induced in E-glass/vinyl ester composite panels subjected to shock blast loading.
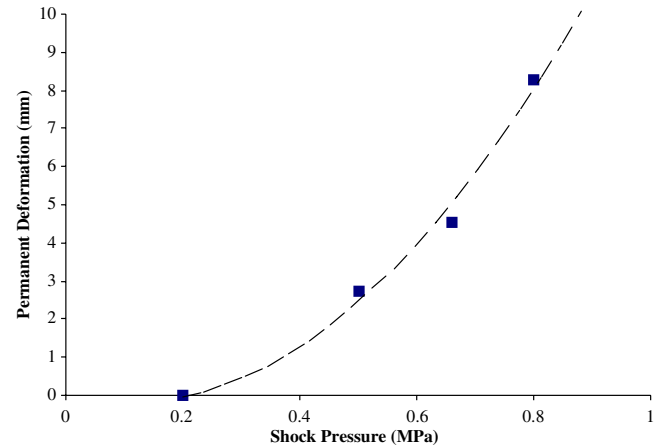

Fig. 7. Plot of center point permanent deformation induced in FGI-1854 composite panels subjected to shock blast loading.

and fiber breakage were observed in the strike face of the panel. All the panels below the threshold shock input suffered no external damage and/or permanent deformation. The threshold level in the FGI-1854 composite was comparatively lower at 0.2 MPa (30 psi). While the FGI-1854 panels had a slow and progressive damage behavior, failure in Devold LT650 was more drastic and rapid. This might suggest that in applications where absolute integrity of structure is needed, Devold LT650 might be more suitable (as long as shock levels are less than the threshold). FGI-1854 panels are more suitable where permanent deformation can be allowed rather than drastic failure; and hence higher shock levels can be absorbed.

6.4. Explosive blast load

6.4.1. Controlled explosion tube – construction

The controlled explosion tube (CET) facility at URI consists of a steel cylindrical tube of outer diameter 76.2 mm (3 in.), inner diameter 25.4 mm (1 in.) and 127 mm (5 in.) long. A schematic of the tube is shown in Fig. 2b. The explosive used in the study consisted of 454 mg of RDX binder and 167 mg of PETN as initial pressing packed in an all plastic case. This ensured that the damage was caused solely due to the explosive blast and not from any fragment impact. The explosive impact was spread over a circular area of 25.4 mm (1 in.) diameter.
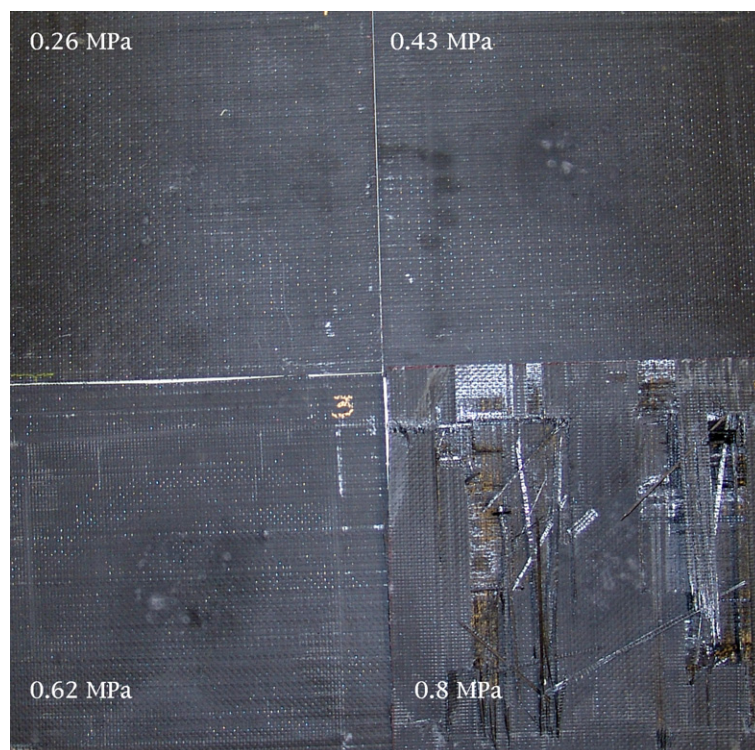

Fig. 8. Strike face damage progression in carbon fiber/vinyl ester composites, subjected to shock blast loading.

6.5. Specimen

The specimens used for explosive blast study were 305 mm (12 in.) square plates of 2.5 mm (0.1 in.) thickness. These plates were fixed on all ends using rigid clamping fixture which exposed a square area of 178 mm × 178 mm (7 in. × 7 in.) to the explosive blast. The end of the CET was flushed against the plate. Again, the plates were also instrumented with strain gages on the rear surface as shown in Fig. 4; similar to those used for the shock tube study.

6.6. Results

The FGI-1854 panels subjected to explosive blast showed extensive strike face delaminations and fiber breakages as shown in Fig. 9a. Also noticeable in these panels were a central burn region which when viewed under a microscope Fig. 10 showed regions devoid of matrix and fiber breakage. The explosive blast produced drastic delam-

ination in strike face of FGI-1854 suggesting inadequate load transfer between the fiber and the matrix under existing high loading rates. In the Devold LT650 panels, damage was observed in the form of fiber breakages on the strike face due to spalling Fig. 9b. The rear face of these panels suffered no external damage. Again, these patterns suggest that FGI-1854 panels have more progressive form of failure whereas damage in Devold LT650 panels is of rapid form.

6.6.1. Strain response

The strain response of all the panels subjected to explosive blast shows a distinct initial compressive pulse, followed by a predominant tensile pulse. The strain response at locations (A) and (B) look similar, due to axisymmetric loading. Fig. 11 plots the initial compressive strain observed in the FGI-1854 and Devold LT650 panels subjected to explosive blast loadings. FGI-1854 panels showed quantitatively more strain since they could deform much more than the Devold LT650 panels.
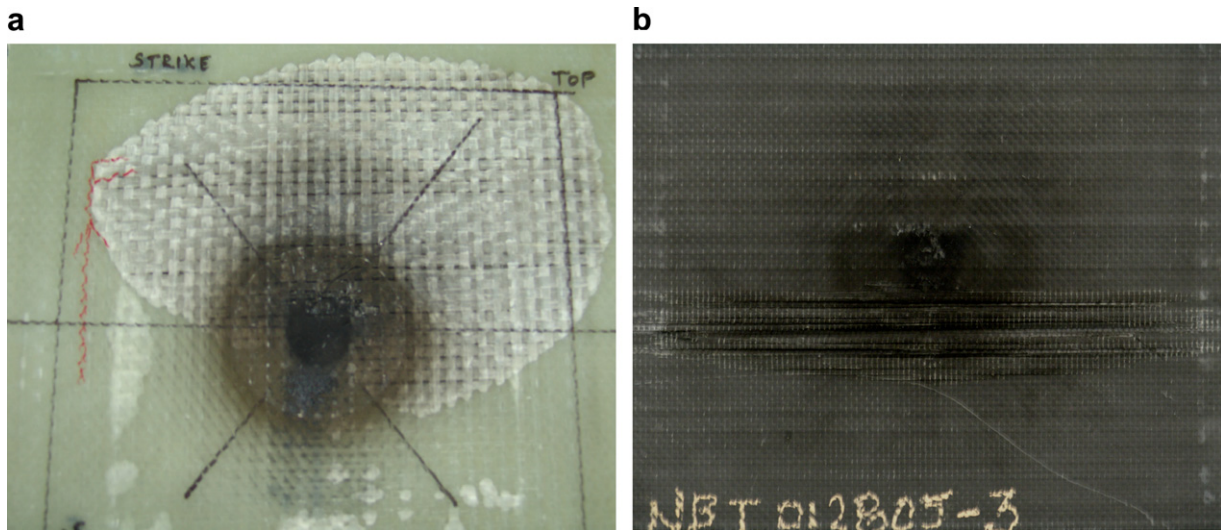
Fig. 9. (a) Damage in strike face of a FGI-1854/vinyl ester composite, subjected to explosive blast loading. Extensive delamination between layers is seen here. (b) Damage in strike face of Devold LT650 carbon fiber/vinyl ester composite.
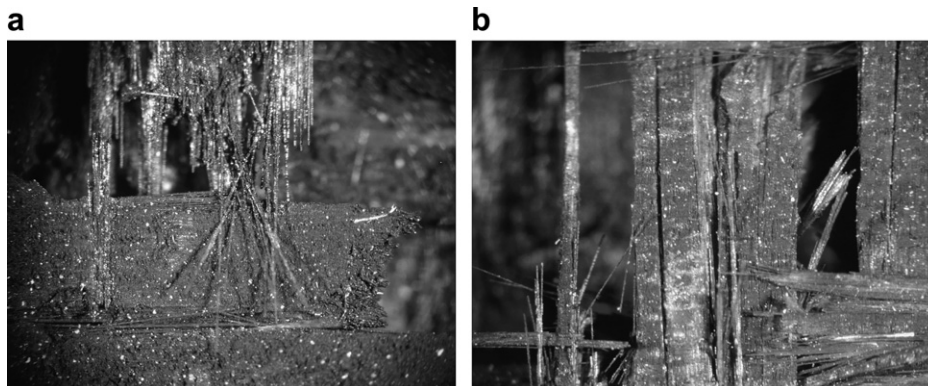
Fig. 10. Central burn region observed in FGI-1854/vinyl ester composites. Extensive fiber breakage and matrix burning are observed in the microscopic view.
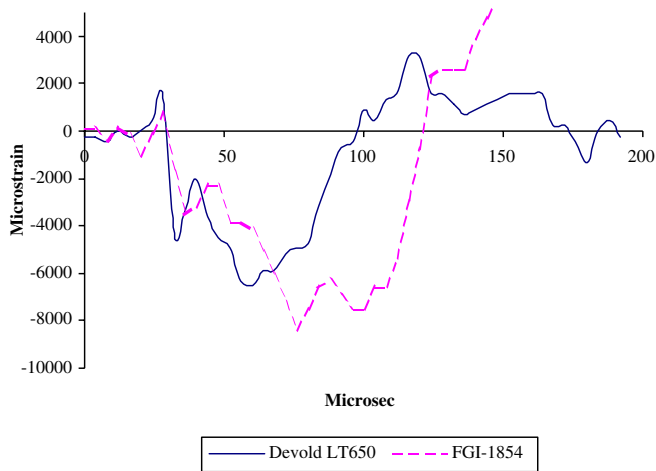
Fig. 11. Initial compressive strain response of Devold LT650 and FGI-1854 composite panels subjected to explosive blast load.

5. Damage patterns as described above were observed in these composite panels when subjected to explosive blast loadings. Whereas E-glass fiber composite showed patches of internal delamination and a central burn region where possible matrix burning is visible, the carbon fiber composites showed fiber breakage and delamination in the strike face. Strain response of these panels show that the carbon fiber panels behave stiffer than the E-glass fiber composite.

Acknowledgements

7. Conclusions

1. The average tensile modulus and the strength of the E-glass fiber composite are 29.2 GPa and 512.5 MPa, respectively in the warp (X_1) direction and 23.9 GPa and 350.9 MPa, respectively in the fill (X_2) direction. The tensile modulus and the strength of carbon fiber composite in warp (X_1) direction are 56.7 GPa and 1125.7 MPa, respectively and in the fill (X_2) direction are 57.1 GPa and 1036.9 MPa, respectively.
2. The compression modulus and the strength of the E-glass fiber composite are 31.9 GPa and 363.4 MPa, respectively in the warp (X_1) direction and 26.9 GPa and 336.4 MPa, respectively in the fill (X_2) direction. The compression modulus and the strength of carbon fiber composite in warp (X_1) direction are 67.5 GPa and 449.7 MPa, respectively and in the fill (X_2) direction are 59.1 GPa and 387.2 MPa, respectively.
3. The in-plane shear modulus and the 0.2% offset strength of the E-glass fiber composite are 4.5 GPa and 44.7 MPa, respectively in the warp (X_1) direction and 4.3 GPa and 47.3 MPa, respectively in the fill (X_2) direction. The in-plane shear modulus and the 0.2% offset strength of carbon fiber composite in warp (X_1) direction are 4.2 GPa and 47.5 MPa, respectively and in the fill (X_2) direction are 3.9 GPa and 45.0 MPa, respectively.
4. When subjected to shock blast loading, the E-glass fiber composite showed continuous damage progression. Various failure modes such as permanent deformation, fiber breakage, and delamination were observed. In contrast, the carbon fiber composites showed no signs of external damage until a certain threshold shock pressure (0.6 MPa) beyond which, the panel failed. Predominant failure modes in these panels were fiber breakage and delaminations in the strike face.

References

[1] Nurick GN, Gelman ME, Marshall NS. Tearing of blast loaded plates with clamped boundary conditions. Int J Impact Eng 1996;18:802–27.
[2] Hammond L, Grzebieta R. Structural response of submerged air-backed plates by experimental and numerical analyses. Shock Vib 2000;7(6):333–41.
[3] Wonderly C, Grenestedt J, Fernlund Göran, Cĕpus Elvis. Comparison of mechanical properties of glass fiber/vinyl ester and carbon fiber/vinyl ester composites. Compos Part B: Eng 2005;36(5):417–26.
[4] Mouritz AP. Ballistic impact and explosive blast resistance of stitched composites. Compos Part B: Eng 2001;32(5):431–9.
[5] Mouritz AP. The damage to stitched GRP laminates by underwater explosion shock loading. Compos Sci Technol 1995;55(4):365–74.
[6] Librescu L, Nosier A. Response of laminated composite flat panels to sonic boom and explosive blast loadings. AIAA J 1990;28(2):345–52.
[7] Lam KY, Lu Chun. Analysis of clamped laminated plates subjected to conventional blast. Compos Struct 1994;29(3):311–21.
[8] Data sheet for Rovcloth 1854, Fiber Glass Industries, 2/2/02.
[9] Product data sheet for LT 650-C12 Biaxial Carbon Product, Devold AMT AS, 10/2/02.
[10] Derakane 510A-40, Product information page, Dow Chemical co.
[11] Smith S, Emmanwori L, Sadler R, and Shivakumar K. Evaluation of composite sandwich panels fabricated using vacuum assisted resin transfer molding. In: SAMPE 2000, Long Beach (CA); May 21–25, 2000.
[12] Sadler R, Sharpe M, Swaminathan G, Shivakumar K. Mechanical properties of panels fabricated by the VARTM processed composites using different fibers and fabric architectures. In: 18th Annual technical conference of ASC, 19–22 October. Gainesville (FL): University of Florida; 2003.
[13] Swaminathan G, Shivakumar K, Sharpe M. Mechanical properties of glass and T700 carbon/vinyl ester composites, developments in theoretical and applied mechanics. In: SECTAM, vol. 22, Tuskegee University, AL; 2004. p. 227–40.
[14] Hsu K, Bernard J, Peters J, Dayal V. Physical basis of tap test as a quantitative imaging tool for composite structures on aircraft. In: Prog. Quantitative NDE, 19, Thompson DO and Chimenti DE. Amer. Inst. Phys., Melville (NY); 2000. p. 2053–60.
[15] Annual Book of ASTM Standards. ASTM International, vol. 15.03, West Conshohocken (PA); 2002.
[16] Abali F, Pora A, Shivakumar K. Modified short beam shear test for measurement of ILSS of carbon–carbon composites. J Compos Mater 2003;37(5):453–64.